Experimental Evaluation of the Performance: A Novel Bi-Facial PV Panel

Tanvir M. Mahim
Electrical and Electronic Engineering
Brac University
Dhaka, Bangladesh
tanvir.mahim@bracu.ac.bd

Adnan Miah
Electrical and Electronic Engineering
Brac University
Dhaka, Bangladesh
adnan.miah@g.bracu.ac.bd

A.H.M.A. Rahim
Electrical and Electronic Engineering
Brac University
Dhaka, Bangladesh
abu.hamed@bracu.ac.bd

Md Rakibul Hasan
Electrical and Electronic Engineering
Brac University
Dhaka, Bangladesh
rakibul.hasan@bracu.ac.bd

Md. Mehedi Hasan Shawon
Electrical and Electronic Engineering
Brac University
Dhaka, Bangladesh
mehedi.shawon@bracu.ac.bd

Tasfin Mahmud
Electrical and Electronic Engineering
Brac University
Dhaka, Bangladesh
tasfin.mahmud@bracu.ac.bd

2023 IEEE Region 10 Symposium (TENSYMP) | 978-1-6654-8258-5/23/$31.00 ©2023 IEEE | DOI: 10.1109/TENSYMP55890.2023.10223485

***Abstract*—Replacement of emission based energy production sources is vital due to the climate change effects in the world. One of the alternatives in this regard is the solar-powered PV cells. This work proposes a novel PV panel design using two mono-facial panels installed back to back to improve power efficiency at reduced space usage. A study was made with an outdoor setup during the winter season for three months, having a single-axis sun-tracking. The findings of this design suggest that the proposed panel gives 22% more power efficiency compared to the mono-facial panel of same dimension. The design was found less expensive compared to conventional bi-facial PV panels. The boost in the power efficiency of the proposed panel design is attributed to the thermal behaviour of the panel, low air pressure-humidity and surface albedo. The findings suggest white concrete surface gives optimal surface albedo for rooftop PV installation.**

Keywords—Renewables, Solar energy, Bi-facial PV panel, Mono-facial PV panel, Single-axis tracking system

I. Introduction

Photovoltaic (PV) is one of the most efficient renewable alternatives to emission based energy. The number of large-scale PV plants and rooftop solar home systems has increased in the last decade. Bi-facial PV panels generate electricity from the front and rear surfaces of the panel. Naturally, they produce more energy than mono-facials [1], [2]. PV plants and rooftop areas with high albedo surfaces use bi-facial. The use of mono-facial panels is high when surface albedo is very poor [3]. Bi-facial is more expensive than mono-facial PV panels. It requires a transparent backsheet (glass) on the rear surface. The backsheet needs to be of high quality to withstand harsh weather and environmental conditions [4]. This increases production costs and specialized mounting systems also increase overall installation costs [5].

The objective of a bi-facial PV plant is to reduce a large portion of the levelized cost of energy with a minimal investment [6], [7]. A performance optimization concern is the quantity of backside irradiance dependent on ground albedo. Due to the indirect irradiation, uniformity of panel rear surface incident irradiation is not straightforward [8].

Johnson evaluated a large-scale grid-tied bi-facial PV system with vertically mounted panels. He addressed the need for better models to estimate the diffuse-reflected radiation and the impact of shading [9]. Kreinin took outdoor measures of bi-facial panels in Jerusalem, Israel. The author proposed a method of determining nominal electrical parameters for each surface of the panel [10]. Yakubu investigated the performance of a bi-facial PV system in Nigeria. He found that bi-facial yields more energy than mono-facial on natural ground surfaces [11]. Singh used commercially available bi-facial and mono-facial modules of the same cell technology in Singapore on a rooftop at the National University of Singapore. He improved the design of bi-facial modules for tropical climate conditions [12]. Janssen presented an outline of a model to calculate the outdoor performance of a bi-facial panel for optical, electrical and thermal aspects in Amsterdam. He identified the optimum bi-faciality factor at different albedos [13]. Obara demonstrated power output characteristics of bi-facial panels using 3kW bi-facial PV systems at a northern snowy area in Kitami City, Hokkaido, Japan [14]. Poulek developed low-concentration PV (LCPV) systems with bi-facial panels [15]. Yusufoglu elaborated on individual and combined effects on the annual energy yield of stand-alone south-facing bi-facial panels by simulations for two site locations with diverse climatic conditions. He found that bi-facial supplies up to 25% more energy as well as 20% excess power efficiency compared to mono-facial [16].

A novel panel design has been presented in this work using two mono-facial panels. An experimental setup for the bi-facial panel was built on a rooftop in the winter months. The objective is to compare the effectiveness of the proposed panel with a mono-facial panel. The proposed panel design shows excellent thermal performance and power efficiency compared to a single mono-facial system.

The organization of this article is: section II describes conventional mono-facial and bi-facial PV, section III briefly explains the simulation of the proposed bi-facial panel, section IV shows the experimental setup of the PV panels, section V analyzes the result and Section VI presents the conclusion of the work.

II. Conventional Mono-facial and Bi-facial PV

The existing mono-facial and bi-facial PV panels with respective electrical PV cell diagrams are presented in this section. PV cells contain semiconductors that convert sunlight to electricity. To reduce reflection and collect electrons released by photons, anti-reflective material and metal conductors cover the PV cells. Mono-facial PV cell efficiency depends on several factors such as incidence of sunlight, temperature of the cells and materials used for the cells.

The mono-facial one-diode PV cell model given in Fig. 1 consists of equivalent series resistance (R_s), parallel resistance (R_{sh}), front surface photocurrent (I_{ph-f}).

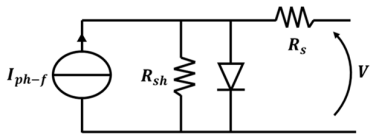

Fig. 1. Mono-facial PV cell one diode model: electrical diagram

The short circuit current of the mono-facial PV cell is shown in (1), which is followed by short-circuit current for the panel [17],

$$I_{sc-f} = I_{ph-f} - I_n[e^{q\left(\frac{V_{oc-f}}{NkT}\right)} - 1] \quad (1)$$

$$I_{sc-m} = A \times I_{sc-f} \quad (2)$$

Here in (2), A is the area of the PV panel in square meters and I_{sc-f} is the short circuit current of the front surface of the PV panel in amperes per square meter. In (1), I_n and q are the diode's reverse saturation current density and an electron's elementary charge, respectively. N, k and T are the ideality factor, Boltzmann constant and junction temperature. The open circuit voltage of the mono-facial PV cell and panel is presented in (3) and (4), respectively [18],

$$V_{oc-f} = \frac{NkT}{q}[\ln(\frac{I_{ph-f}}{I_{ph0} + I_0})] \quad (3)$$

$$V_{oc-m} = A \times V_{oc-f} \quad (4)$$

In (4), V_{oc-f} is the open circuit voltage of the front surface of the PV panel in volts per square meter. In (3) I_{ph0} and I_0 are the diode saturation current in the absence of light and the diode reverse saturation current.

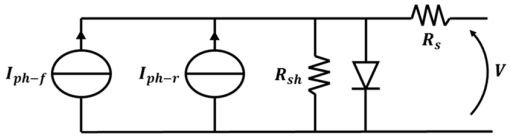

Fig. 2. Bi-facial PV cell one diode model: electrical diagram

Fig. 2 represents the bi-facial one-diode PV cell model. The cell structures are identical for both the front and rear sides of the panel. The bi-facial cell captures the reflected sunlight from surfaces such as ground and buildings. To reduce reflection from panel surfaces and pass sunlight through the rear side of the bi-facial cell, a reflective coat and a layer of transparent conductive material cover the PV cell. This allows sunlight to reach the front surface through the back of the cell. Several factors such as angle and intensity of sunlight, albedo and the cell's temperature, influence bi-facial power efficiency. Here albedo is the reflectivity of surfaces such as grounds and buildings.

The sum of photocurrent of the front and rear surfaces for bi-facial is the same as that of a mono-facial cell with two current sources. One for each surface given in Fig. 2. The resultant panel current calculation is a simple sum of front and rear surface currents. The bi-facial PV cell and panel short circuit current is given in (5) and (6), respectively [19],

$$I_{sc-ref} = I_{sc-f} + I_{sc-r} \quad (5)$$

$$I_{sc-b} = A \times I_{sc-ref} \quad (6)$$

Calculation of the total voltage uses front and rear surface open circuit voltage. The total bi-facial PV cell and panel open-circuit voltage is presented in (7) and (8) [20],

$$V_{oc-ref} = V_{oc-f} + \frac{(V_{oc-r} - V_{oc-f}) \times \ln(R_{I_{sc}})}{\ln(\frac{I_{sc-r}}{I_{sc-f}})} \quad (7)$$

$$V_{oc-b} = A \times V_{oc-ref} \quad (8)$$

Where $R_{I_{sc}}$ is the gain of short-circuit current relative to the panel's front-side illumination. Using short circuit current, open circuit voltage and FF (fill factor), the maximum power equation is [21],

$$P_{mpp} = I_{sc} \times V_{oc} \times FF \quad (9)$$

The maximum power calculation for both bi-facial and mono-facial is similar. In (5), FF is the ratio of the maximum power output of the panel to the product of its open-circuit voltage and short-circuit current.

The energy [18] and power efficiency [20] calculation of the PV panels use the following equations

$$E = P_{mpp}(\frac{T}{1000})A \times H \quad (10)$$

$$\eta = \frac{P_{mpp}}{G_{p_{0a}} cos\theta[1 - A(\frac{T_c - T_{c-stc}}{800})]} \times 100\% \quad (11)$$

In the above, T and H are the total amounts of panel exposure time to sunlight and the average solar irradiance on the panel, respectively. Equation (11) gives the power efficiency of a panel where, $G_{p_{0a}}$ and θ are the plane of array irradiance and the angle of incidence, respectively. T_c and T_{c-stc} are the temperature of the cell and standard test condition temperature, respectively.

III. Simulation of the Proposed Bi-facial Panel

A novel bi-facial panel design is proposed in this section. Here the simulation is done experimentally. A brief schematic of the experimental setup including the proposed panel is shown in Fig. 4a. An identical-sized mono-facial panel was also used to compare the efficiency of the proposed panel presented in Fig. 4c.

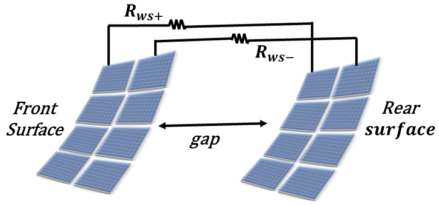

Fig. 3. Proposed bi-facial panel design

Fig. 3 presents the proposed bi-facial panel where two mono-facial panels are connected in parallel. Each panel has the same dimension. The panels are installed back to back, making one mono-facial the front surface and the other the rear surface for the proposed bi-facial panel. The R_{ws+} and R_{ws-} are the positive and negative terminal wire resistance respectively. There is a gap between the front and rear surfaces of the proposed panel that is absent in conventional PV panels.

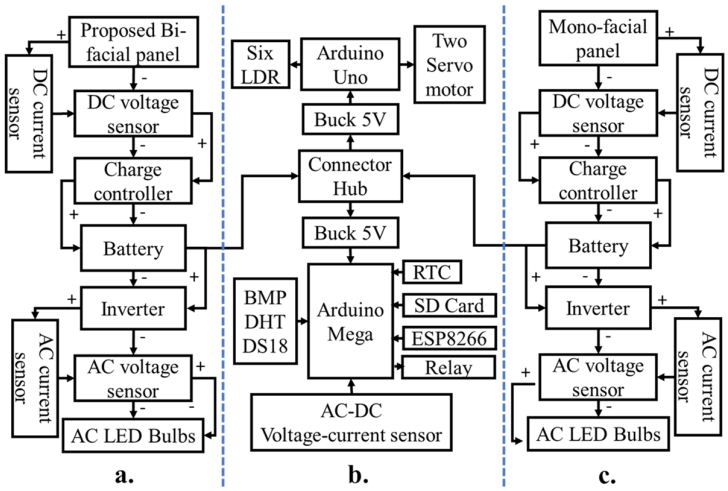

Fig. 4. Experimental setup: a) proposed bi-facial panel b) control units c) mono-facial panel

Fig. 4a shows the experimental setup of the proposed bi-facial panel. This is compared with a single mono-facial panel given in Fig. 4c. Here both panels have the same dimension. A single-axis tracking system has been used to increase the power efficiency of both panels in the system. The system contains charge controllers, DC voltage and current sensors, a single-phase inverter and AC loads. The loads have similar ratings for both panels. Fig. 4b shows the connection diagram of the control unit for the experimental setup. It controls the data storing flow for both panels and the tracking system. The data collection flowchart for the system is shown in Fig. 5. It depicts the data flow from collection to storing using NodeMCU which is an IoT device. According to Fig. 4 and Fig. 5, the experimental setup is developed as given in the next section.

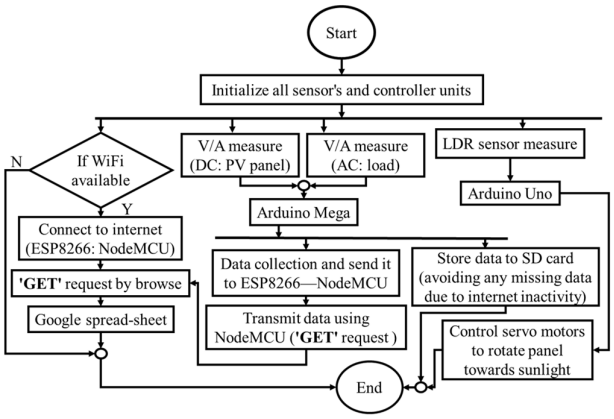

Fig. 5. Data collection flowchart

IV. The Experimental Setup

Fig. 6 gives a view of the experimental setup of the system given in Fig. 4. The experiment was performed in the winter of 2022-23. The setup consists of the following: two identical-sized PV panels supported by a single-axis tracking system shown in Fig. 6b, one for mono-facial, and the other one is proposed bi-facial. The modification of the proposed panel uses two identical-sized mono-facial panels installed with parallel connections, with one panel at the front side and the other at the rear side.

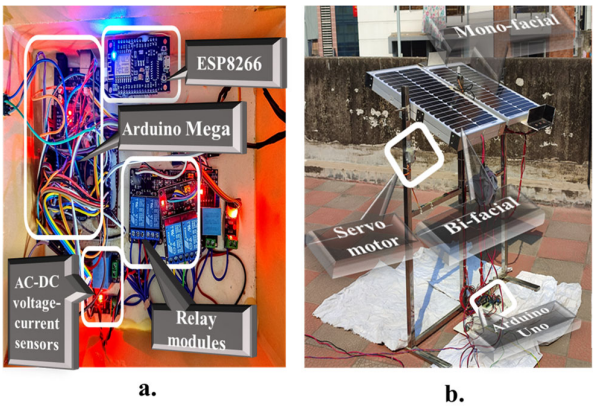

Fig. 6. a) Monitoring system b) Single-axis sun-tracking

Weather parameters such as ambient temperature, humidity and air pressure; PV panel parameters mainly voltage, current and temperature were recorded. As the system runs on AC loads, PV output connects to charge controllers to maintain stable voltage levels. The charge controller is connected to the battery followed by an inverter. The inverter is then connected to the AC loads. To monitor the DC voltage and current in the PV panels. The DC voltage and current sensors were used to monitor the voltage and current in the circuit. The ratings of the panels are given in Table I. Here the proposed bi-facial panel's parameters are measured and the mono-facial panel's parameters are rated. The dimension of both panels is 0.44 m^2.

TABLE I. Panel Ratings

Panel	Parameter	Rating
Mono-facial (commercial)	Maximum power (P_{mpp})	20 W
	Open circuit voltage (V_{oc-m})	22 V
	Short circuit current (I_{sc-m})	1.4 A
	Maximum power voltage (V_{mp-m})	17.5 V
	Maximum power current (I_{mp-m})	1.14 A
Proposed panel (bi-facial)	Maximum power (P_{mpp})	34 W
	Open circuit voltage (V_{oc-b})	22 V
	Short circuit current (I_{sc-b})	2.15 A
	Maximum power voltage (V_{mp-b})	17.5 V
	Maximum power current (I_{mp-b})	1.94 A

Table II provides a list of the sensors and devices used in the experimental setup. A brief description of the function of each is included. The sensors used for the first objective of the table, monitor the AC and DC power of the setup. NodeMCU and Arduino Uno are used for WiFi connectivity and single-axis tracing of the panels in the setup. An onboard real-time clock is used to track the date and time of the data that is recorded.

TABLE II. DEVICES AND SENSORS

Objective	Sensors
Power	0-25V Voltage Sensor Module ACS712 Current Sensor AC Voltage Sensor Module ZMPT101B (Single Phase) ACS712 Current Sensor
The Control unit	Arduino mega ESP8266 (NodeMCU) Arduino Uno
Onboard clock	DS1307 RTC Module
Data security	MicroSD Card Module
Switching	2 Channel 5V Relay Board Module
Panel temperature	DS18B20
Weather parameters	DHT22 BMP180
Sun Tracking	LDR 20mm sensors ROB5GRHS3115
Power management	LM2596 DC-DC BUCK CONVERTER

A load-handling system was designed. It uses two double-channel relays connected with AC voltage and current sensors at the input and output of the system given in Fig. 6a. It contains the control unit and data transmission unit. The control unit receives and sends all the sensor data to the IoT device. The IoT device then transmits the data to a Google sheet using a GET request with a pattern "https://script.google.com/…..". Entering the pattern into a web browser of Google's server responds by asking the browser to redirect to another URL with the domain "script.googleusercontent.com" with a new GET request [22]. GET is a type of HTTP (Hypertext Transfer Protocol) request that extracts data from a source with the help of the internet. A micro SD card module was used to ensure that the data is stored offline to avoid missing data due to the WiFi module's network disturbance.

Arduino Uno was used to control the single-axis tracking system. The servo motors were controlled using the LDR sensors (Fig. 6b). The experimental setup contains two buck converters to distribute the power evenly throughout the sensors and devices as given in Fig. 4.

The control units used for data processing are depicted in Table III. Here communication protocols that were used are I2C for LCDs and BMP180, Single bus for DHT22, One-wire bus for DS18B20, and SD and SPI bus for SD-card module.

TABLE III. DATA PROCESSING

Controller unit	Devices
Arduino Mega	LCDs BMP180 DHT22 DS18B20 SD-card module
ESP8266	WIFI

For the experimental setup, a white-colored concrete surface was chosen since it has the highest albedo value of $\alpha = 0.67$ for rooftop surfaces.

Fig. 7 shows the trend of energy from the PV panel. It was found that the energy trend of the proposed panel consistently produces approximately 45% extra energy compared to mono-facial PV for the period Nov 22 – Jan 23. During December it was noticed that energy generation fluctuates each day because of the foggy weather conditions of the winter season. The average hourly energy generation for each day for mono-facial and bi-facial PV panels is also shown.

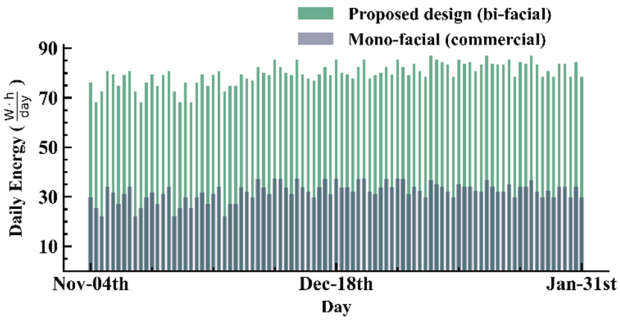

Fig. 7. PV panel energy variation (winter season: Nov 2022 – Jan 2023).

V. ANALYSIS OF THE RESULT

An analysis of the data recorded is presented in this section. Comparative power efficiency analysis of the proposed bi-facial and mono-facial panels is presented. Correlation analysis of the proposed bi-facial panel is evaluated.

A. Power Efficiency of PV Panels

The power efficiency is derived from the monthly mean power of the PV panels. SVR (support vector regressor) was used to analyze the power efficiency of the panels. The efficiency of the proposed design is based on the experimental data that was recorded.

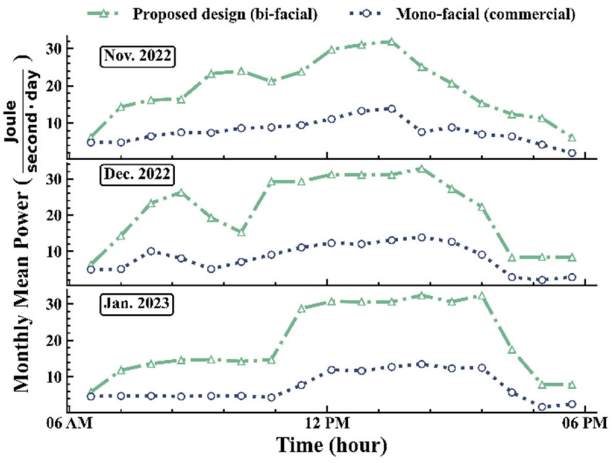

Fig. 8. PV panels power (Monthly Mean power)

Fig. 8 Shows the monthly mean power recorded from the experimental setup during winter for both the mono-facial and proposed bi-facial panel. A consistent power gain is observed

with the bi-facial compared to the mono-facial. The sharp dips in power for the panels are due to cloud cover. In December, the panels received high irradiance due to the availability of a more extended period of sunlight per day. In January, from the morning to late noon, the power generation of panels was low due to the foggy weather conditions of the winter season.

Statistical analysis was done using SVR (support vector regressor). The SVR function employed is [23],

$$f(x) = \sum_{i=1}^{n} (\alpha_i - \alpha_i^*) k(x_i, x) + b \qquad (12)$$

Here, x is the input to the function; α_i and α_i^* are the Lagrange multipliers; k, n and b are the kernel function, the number of training instances and the y-axis intercept of the regression line, respectively.

Fig. 9 shows the best-fit line for the experimental efficiency scatter points found by SVR. It was observed that the proposed bi-facial design is approximately 22% more efficient than the mono-facial one for the entire duration of the experiment. Considering only the noon period, the proposed design gives 30% more efficiency than mono-facial.

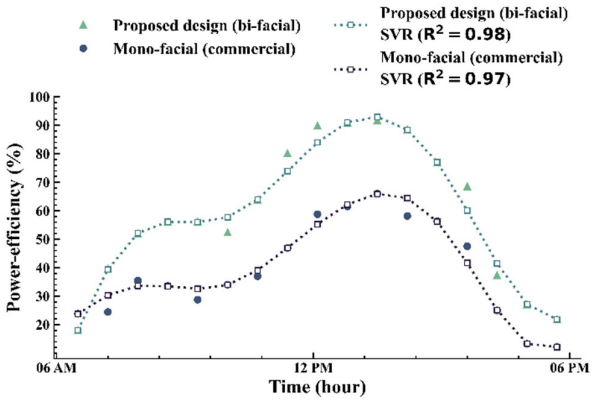

Fig. 9. Panel efficiency (monthly mean)

B. *Observation of the Relationship between PV Power and Weather Parameters*

The correlation between the weather parameters and the PV power recorded through the experimental setup is analyzed in this section.

The correlation effect of the parameters is compared with PV power. Fig. 10 shows the weather parameter's effects on the temperature of the panels. The proposed panel maintains a lower temperature compared to the mono-facial panel due to its simple design feature—a gap between the two panels. This gap provides continuous air ventilation between the front and rear sides.

The ambient temperature given in Fig. 10a shows a strong positive linear correlation with the proposed panel's power in Fig. 11. It also shows that humidity has a strong negative linear correlation with ambient temperature. This correlation is found using the Pearson correlation coefficient. The Pearson correlation coefficient is [23],

$$r = \frac{(n\sum XY - \sum X \sum Y)}{\sqrt{\{n\sum x^2 - (\sum x)^2\}\{n\sum Y^2 - (\sum Y)^2\}}} \qquad (13)$$

Here n, $\sum X$ and $\sum Y$ are the number of observations, the sum of the deviations of X from its mean and the sum of the deviations of Y from its mean respectively.

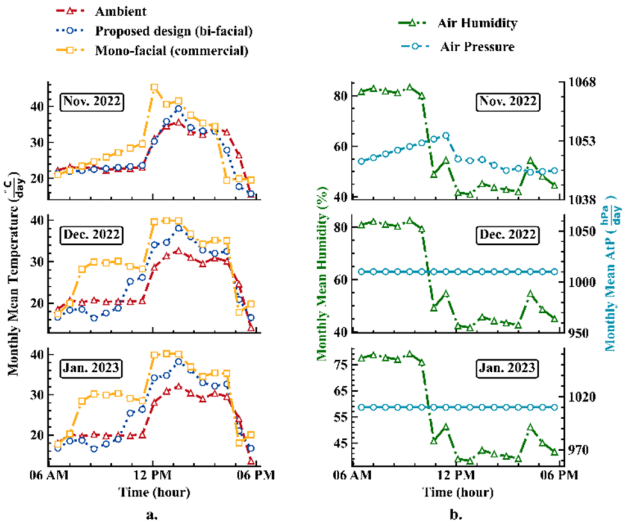

Fig. 10. Weather parameter relation to panel temperatures (monthly mean) for a) ambient temperature and b) Air pressure-humidity

Fig. 11 also shows that air pressure shown in Fig. 10b has a weak negative correlation with ambient temperature but has a non-linear or monotonic relationship. This correlation is determined using Spearman's rank correlation coefficient. The Spearman's rank correlation coefficient is [23],

$$\rho = 1 - \frac{6\sum d_i^2}{n(n^2 - 1)} \qquad (14)$$

Here d and n are the differences between the ranks of corresponding values of the two variables and the number of observations.

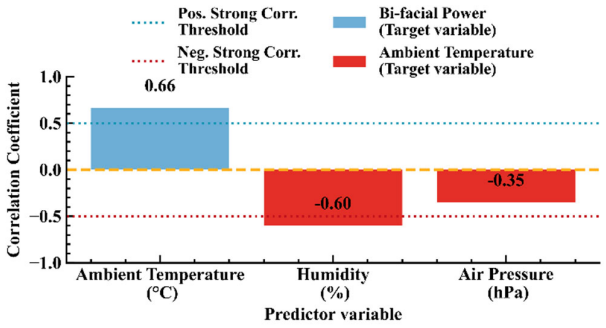

Fig. 11. Proposed panel correlation with weather parameters

From the correlation analysis, it is found that the ambient temperature's direct positive linear correlation to the proposed PV panel power is indirectly dependent on air pressure and humidity.

C. Cost Analysis of the Proposed Bi-facial Panel

The proposed panel design is about 52.07% (estimated) less expensive than conventional bi-facial panels. Table IV shows that the proposed bi-facial panel is more cost-effective than the conventional bi-facial. It also shows that the proposed panel is 43.81% more than the conventional mono-facial panel. The conventional mono-facial and bi-facial panel prices are taken from references [5], [24] and [1], [7] respectively.

TABLE IV. PRICE COMPARISON OF THE PROPOSED DESIGN WITH EXISTING PANELS

Continent	Panel prices ($)		
	Mono-facial (commercial)	***Bi-facial (commercial)***	***Proposed design (bi-facial)***
North America	105	315	151
Europe	87.5	245	138
Asia-Africa	70	210	126

In Table IV all the panels have a similar dimension of $1{,}98m^2$. The watt rating of the mono-facial panel is 350W [24]and the bi-facial panel is 420W [4], [23]. The estimated rating of the proposed bi-facial is 422W.

VI. CONCLUSION

A novel bi-facial PV panel design has been presented in this work. The bi-facial panel is constructed connecting two mono-facials back to back. Statistical analysis of the recorded data shows that the proposed bi-facial scheme gives 22% higher efficiency compared to the existing mono-facial systems. This increase in efficiency is attributed to the lower temperature of the panels in the proposed scheme. The boost in efficiency is also because of the high albedo of the white rooftop.

The proposed design has also been observed to be less expensive compared to the bi-facial panels available in the market.

ACKNOWLEDGMENT

This work was performed by Brac University EEE ATC Project Team 2 during the 2022 academic year. The team members appreciate Brac University's support in completing the project.

REFERENCES

[1] "Bifacial Solar Panels - The Ultimate Guide (2023)." https://www.waaree.com/blog/bifacial-solar-panels (accessed Mar. 11, 2023).

[2] G. Raina and S. Sinha, "Experimental investigations of front and rear side soiling on bifacial PV module under different installations and environmental conditions," *Energy for Sustainable Development*, vol. 72, pp. 301–313, Feb. 2023, doi: 10.1016/J.ESD.2023.01.001.

[3] C. A. Gueymard, V. Lara-Fanego, M. Sengupta, and Y. Xie, "Surface albedo and reflectance: Review of definitions, angular and spectral effects, and intercomparison of major data sources in support of advanced solar irradiance modeling over the Americas," *Solar Energy*, vol. 182, pp. 194–212, Apr. 2019, doi: 10.1016/J.SOLENER.2019.02.040.

[4] R. Guerrero-Lemus, R. Vega, T. Kim, A. Kimm, and L. E. Shephard, "Bifacial solar photovoltaics – A technology review," *Renewable and Sustainable Energy Reviews*, vol. 60, pp. 1533–1549, Jul. 2016, doi: 10.1016/J.RSER.2016.03.041.

[5] "SEIA | Solar Energy Industries Association." https://www.seia.org/ (accessed Mar. 11, 2023).

[6] G. Razongles *et al.*, "Bifacial Photovoltaic Modules: Measurement Challenges," *Energy Procedia*, vol. 92, pp. 188–198, Aug. 2016, doi: 10.1016/J.EGYPRO.2016.07.056.

[7] "Bifaciality: One small step for technology, one giant leap for kWh cost reduction - PV Tech." https://www.pv-tech.org/technical-papers/bifaciality-one-small-step-for-technology-one-giant-leap-for-kwh-cost-reduction/ (accessed Mar. 12, 2023).

[8] L. Kreinin, A. Karsenty, D. Grobgeld, and N. Eisenberg, "PV systems based on bifacial modules: Performance simulation vs. design factors," *2017 IEEE 44th Photovoltaic Specialist Conference (PVSC)*, vol. 2016-November, pp. 2688–2691, Nov. 2016, doi: 10.1109/PVSC.2016.7750138.

[9] J. Johnson, D. Yoon, and Y. Baghzouz, "Modeling and analysis of a bifacial grid-connected photovoltaic system," *IEEE Power and Energy Society General Meeting*, 2012, doi: 10.1109/PESGM.2012.6345266.

[10] L. Kreinin, N. Bordin, A. Karsenty, A. Drori, D. Grobgeld, and N. Eisenberg, "PV module power gain due to bifacial design. Preliminary experimental and simulation data," *2010 35th IEEE Photovoltaic Specialists Conference*, pp. 2171–2175, 2010, doi: 10.1109/PVSC.2010.5615874.

[11] R. O. Yakubu, L. D. Mensah, D. A. Quansah, M. S. Adaramola, and Y. Hammed, "Performance evaluation of bifacial solar PV modules under different climatic regions in Nigeria," *E3S Web of Conferences*, vol. 354, p. 02006, 2022, doi: 10.1051/E3SCONF/202235402006.

[12] H. K. Singh, M. Mathew, A. Kottantharayil, and C. S. Solanki, "Performance Investigation of Bifacial PV Modules in the Tropics," *27th European Photovoltaic Solar Energy Conference and Exhibition*, no. 3-936338-28–0, pp. 3263–3266, Oct. 2012, doi: 10.4229/27THEUPVSEC2012-4BV.2.15.

[13] G. J. M. Janssen, B. B. Van Aken, A. J. Carr, and A. A. Mewe, "Outdoor Performance of Bifacial Modules by Measurements and Modelling," *Energy Procedia*, vol. 77, pp. 364–373, Aug. 2015, doi: 10.1016/J.EGYPRO.2015.07.051.

[14] S. Obara, N. Ishikawa, and K. Sugibuchi, "Bifacial-PV Power Output Gain in the Field Test Using '"EarthON"' High Bifaciality Solar Cells," *28th European Photovoltaic Solar Energy Conference and Exhibition*, pp. 4312–4317, Nov. 2013, doi: 10.4229/28THEUPVSEC2013-5BV.7.72.

[15] V. Poulek, A. Khudysh, and M. Libra, "Innovative low concentration PV systems with bifacial solar panels," *Solar Energy*, vol. 120, pp. 113–116, Oct. 2015, doi: 10.1016/J.SOLENER.2015.05.049.

[16] U. A. Yusufoglu, T. M. Pletzer, L. J. Koduvelikulathu, C. Comparotto, R. Kopecek, and H. Kurz, "Analysis of the Annual Performance of Bifacial Modules and Optimization Methods," *IEEE J Photovolt*, vol. 5, no. 1, pp. 320–328, Jan. 2015, doi: 10.1109/JPHOTOV.2014.2364406.

[17] M. E. Ropp and S. Gonzalez, "Development of a MATLAB/Simulink Model of a Single-Phase Grid-Connected Photovoltaic System," *IEEE Transactions on Energy Conversion*, vol. 1, no. 24, pp. 195–202, 2009, doi: 10.1109/TEC.2008.2003206.

[18] R. A. Messenger and A. Abtahi, "Photovoltaic Systems Engineering," *Photovoltaic Systems Engineering*, Sep. 2018, doi: 10.1201/9781315218397.

[19] R. G. , Jr. Ross, Ross, R. G., and Jr., "Flat-plate photovoltaic array design optimization," *pvsp*, pp. 1126–1132, 1980, Accessed: Mar. 10, 2023. [Online]. Available: https://ui.adsabs.harvard.edu/abs/1980pvsp.conf.1126R/abstract

[20] J. Libal and R. Kopecek, "Bifacial Photovoltaics : technology, applications and economics," p. 304.

[21] "PVEducation." https://www.pveducation.org/ (accessed Mar. 09, 2023).

[22] "How to post data to Google sheets using ESP8266 | Embedded Lab." https://embedded-lab.com/blog/post-data-google-sheets-using-esp8266/ (accessed Mar. 08, 2023).

[23] T. Hastie, R. Tibshirani, and J. Friedman, "The Elements of Statistical Learning," 2009, doi: 10.1007/978-0-387-84858-7.

[24] "National Renewable Energy Laboratory (NREL) Home Page | NREL." https://www.nrel.gov/ (accessed Mar. 11, 2023).